Journal of Molecular Catalysis A: Chemical 316 (2010) 106–111

Contents lists available at ScienceDirect

Journal of Molecular Catalysis A: Chemical

journal homepage: www.elsevier.com/locate/molcata

Computational study of the properties and metathesis activity of Mo methylidene species in HZSM-5 zeolite

Jarosław Handzlik*

Institute of Organic Chemistry and Technology, Cracow University of Technology, ul. Warszawska 24, PL 31-155 Kraków, Poland

ARTICLE INFO

Article history:
Received 8 October 2008
Received in revised form 1 October 2009
Accepted 5 October 2009
Available online 12 October 2009

Keywords:
ZSM-5
Molybdenum
Metathesis
DFT
Methylidene

ABSTRACT

Four different cluster models of Mo(VI) methylidene centres in the HZSM-5 framework are investigated with DFT. The positive charge on the $MoO(CH_2)$ fragment is higher for the Mo centre with two Al atoms in its vicinity, compared to the models with only one Al site. The activity of two selected Mo centres is examined by the calculation of the pathway of ethene metathesis. In both cases the cycloaddition of ethene to the Mo methylidene centre proceeds easily. On the other hand, the cycloreverse step involves a relatively high energy barrier for the Mo centre with one Al site in the vicinity, whereas the barrier is low for the model with two T sites occupied by Al atoms. Moreover, the key molybdacyclobutane intermediate is a thermodynamically stable species in the first case, but it is unstable in the second case. Thus, a high metathesis activity is predicted if two Brønsted acid sites are replaced by the Mo centre. A secondary molybdacyclobutane structure can be formed as well, but this species is less stable than the primary metallacycle.

1. Introduction

Supported metal oxide catalysts are applied in large-scale industrial processes involving metathesis of alkenes [1,2]. It is well recognised for rhenium oxide catalysts that higher acidity of the support favours their metathesis activity [2–4]. After replacement of the acidic hydroxyl groups by rhenium oxide species, electron-poor rhenium centres are formed which are the precursors of the active sites. In the case of the heterogeneous Mo catalysts, the relationship between the support properties and metathesis activity is not so straightforward, because of more complex chemistry of surface molybdenum species, compared to the rhenium species. Therefore, the properties of the supported Mo catalysts are strongly dependent on a number of factors, involved in the preparation and activation processes [2,5–12]. However, if variously supported Mo catalysts are prepared in the same manner, molybdena–silica–alumina systems exhibit better activity than the catalysts synthesized using alumina or silica, which are less acidic than silica–alumina [10–12]. One can expect that Mo species located in the zeolite framework are also able to catalyze alkene metathesis. Indeed, Mo/HY [10] and Mo/HBeta [13] systems were reported to be active in metathesis of C_2–C_4 alkenes. Our recent experimental studies showed that Mo/HZSM-5 catalyst can be effective in propene metathesis as well [14].

The carbene mechanism [15,16] of olefin metathesis, involving metal alkylidene and metallacyclobutane species, was confirmed by a number of computational studies, for both homogeneous [17–23] and heterogeneous systems [24–29]. The previous theoretical investigations of molybdena–alumina and molybdena–silica catalysts showed that a specific location of Mo alkylidene species on the support is decisive for their high metathesis activity [25–29]. Both local electronic properties of the support and geometry of the active site strongly affect the activity.

This paper is a continuation of the previous theoretical studies of supported Mo catalysts active in olefin metathesis [25–29]. In the present work, Mo(VI) methylidene sites in the ZSM-5 framework are modelled. Similarly to the earlier works [25,26,28,29], density functional theory and cluster models are applied. Electronic and geometrical properties of the considered Mo methylidene species are discussed. The activity of two selected Mo centres is examined by the calculation of the pathway of ethene metathesis.

2. Computational details

The cluster models containing 8, 11 and 12 tetrahedral sites (T sites) are cut off from the orthorhombic ZSM-5 structure [30]. The dangling bonds have been saturated with hydrogens replacing the removed T sites. The use of finite clusters to study the activity of the Mo species in the zeolite framework is justified by the local nature of both support relaxation and the considered chemical interactions. The cluster approach was applied in a number

* Tel.: +48 12 6282196; fax: +48 12 6282037.
E-mail address: jhandz@pk.edu.pl.

1381-1169/$ – see front matter © 2009 Elsevier B.V. All rights reserved.
doi:10.1016/j.molcata.2009.10.007

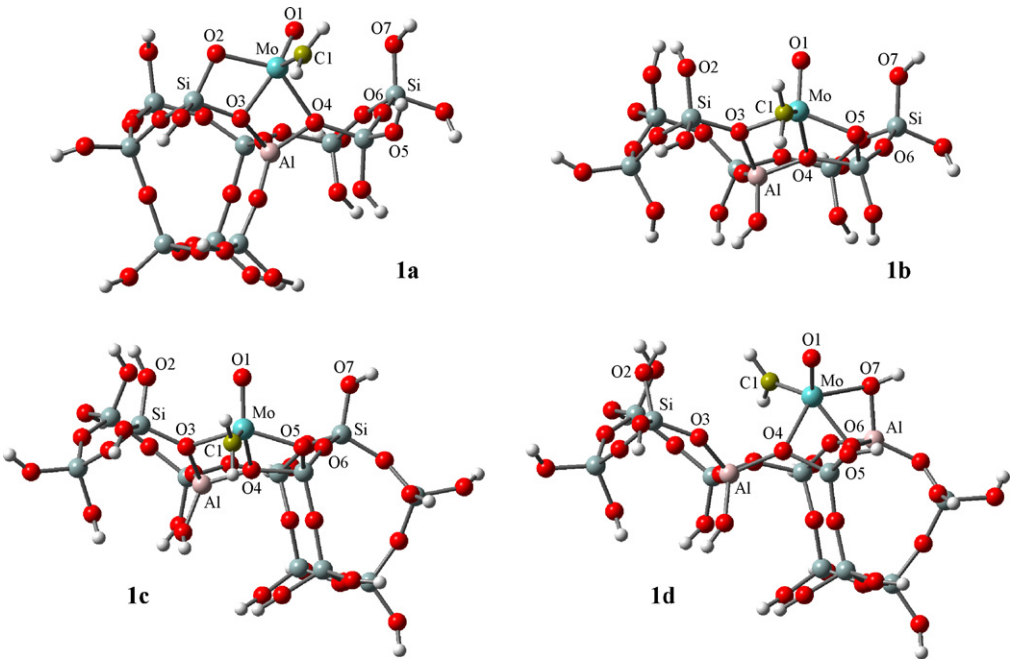

Fig. 1. Models of the Mo methylidene centres in HZSM-5.

of other computational studies concerning the catalysts based on ZSM-5 [31–35].

There are 12 crystallographically distinct T sites in the orthorhombic ZSM-5 framework and the position of Al atoms is still a subject under debate [35–41]. In this work, T2 and T6 sites have been chosen for the location of Al, in accordance with other authors [35,38–40]. Respective structures of the Mo centres have been attached to the clusters.

The calculations have been performed at the hybrid DFT level, using the B3LYP functional [42,43]. The LANL2DZ basis set, including the Hay–Wadt effective core potential [44] is applied for molybdenum, whereas other atoms are described by the Dunning-Huzinaga full double-ζ basis set [45]. This basis combination is used for the geometry optimisation carried out by employing the Berny algorithm with redundant internal coordinates [46]. The positions of the bottom atoms of the zeolite cluster and all the terminating hydrogens were frozen during the geometry optimisation. The potential energy minima and the localised transition states are confirmed by the analysis of the harmonic vibrational frequencies. The zero-point energy corrections are calculated for each structure. Single point energy calculations for the optimised structures have been performed using the LANL2DZ basis set for molybdenum and the D95(d,p) basis set for other atoms. At this level of theory, electronic properties of the active Mo centres have been also analysed, by using the Mulliken population analysis (MPA) [47], the natural population analysis (NPA) [48,49] and the Mayer bond-order indices [50]. This methodology was successfully applied in the previous works on supported Mo catalysts for alkene metathesis [25,26,28,29].

All of the calculations have been done with the GAUSSIAN 03 suite of programs [51]. For the graphic presentation of the systems, the GaussView 4.0 software [52] has been used.

3. Results and discussion

3.1. Models of surface Mo methylidene sites

Four different models of the Mo(VI) methylidene centres in HZSM-5 are proposed (Fig. 1). All clusters include the same two 5T rings connected to each other by a common Si–O–Al bridge. In the starting geometries, the molybdenum was pseudo-tetrahedrally coordinated, analogously to the active metathesis sites on alumina [25–27] and silica [28,29]. The Mo atom was twofold bonded to the surface. After the geometry optimisation, the molybdenum is threefold bonded to the surface and possesses one methylidene ligand and one oxo ligand.

In the first structure, **1a**, the Mo centre is attached to a 11T cluster, in which one T site (T2 in the initial geometry) is occupied by aluminium. The structures **1b** and **1c** represent the same Mo methylidene site, but the latter cluster is more advanced. In both cases, one Al site is present in the model. Finally, in the system **1d**, two T sites (T2 and T6) are occupied by Al atoms. This is the only difference between the zeolite fragments of the structures **1c** and **1d** (Fig. 1).

The concentration of Al–O–Si–O–Al pairs (model **1d**) in the ZSM-5 framework depends on the Si/Al ratio [53–55]. A stochastic simulation indicated a significant fraction of Al atoms situated at these sites [53]. On the other hand, experimental investigations showed that the distribution of Al atoms in the ZSM-5 framework is not controlled by statistical rules but is influenced by the synthesis procedure [41,54]. The fraction of Al atoms in the Al–O–Si–O–Al sequences is rather low or negligible in typical ZSM-5 materials, but this fraction is significant for ZSM-5 zeolite with an unusually high Al concentration (Si/Al = 8.1) [55]. Al–O–Si–O–Al sites were also assumed in a number of theoretical models describing ZSM-5-based catalytic systems [31–34].

The lengths of the carbene bond are very similar for all of the models proposed, but the Mo=C bond-order for the centre **1d** is a little lower than in the case of the other systems (Table 1). Generally, the presently calculated Mo=C distances are very close to the carbene bond lengths predicted for metathesis-active Mo sites on alumina [25,26] and silica [28,29] as well as are similar to those calculated for Mo methylidene sites in HBeta zeolite [56,57]. The lengths and orders of formally double Mo=O bonds for **1a**–**1c** systems are almost identical to each other, while the corresponding bond for **1d** is a bit stronger. This can be understood by the fact that the average strength of the single Mo–O bonds is lower for the latter model, compared to the rest of the systems (Table 1).

Table 1
Selected atomic distances *R* (Å) and bond orders *P* for the Mo methylidene species.

	1a		1b		1c		1d	
	R	*P*	*R*	*P*	*R*	*P*	*R*	*P*
Mo–C1	1.895	1.64	1.899	1.64	1.897	1.65	1.896	1.60
Mo–O1	1.705	2.08	1.704	2.07	1.704	2.08	1.695	2.15
Mo–O2	2.084	0.76	–	–	–	–	–	–
Mo–O3	2.051	0.48	2.173	0.43	2.151	0.40	–	–
Mo–O4	2.255	0.39	2.137	0.45	2.127	0.45	2.272	0.51
Mo–O5	–	–	2.048	0.77	2.035	0.78	–	–
Mo–O6	–	–	–	–	–	–	2.088	0.49
Mo–O7	–	–	–	–	–	–	2.292	0.43

Table 2
Selected charges for the Mo methylidene species.

	1a		1b		1c		1d	
	MPA	NPA	MPA	NPA	MPA	NPA	MPA	NPA
q(Mo)	1.33	1.52	1.31	1.49	1.32	1.50	1.25	1.47
q(C1)	−0.64	−0.51	−0.60	−0.46	−0.63	−0.50	−0.54	−0.36
q($MoOCH_2$)	0.71	0.97	0.71	0.98	0.70	0.95	0.80	1.14

One can also notice that both the geometries and bond indices are almost the same for the sites **1b** and **1c**, despite the fact that **1b** is a simplified variant of **1c**.

In Table 2, charges obtained by the Mulliken and natural population analyses are listed. While the values given by each method are obviously different, the same trends are observed. It can be noticed that the respective charges for the systems **1a**–**1c** are quite similar to each other but those for **1d** are more different. Especially, the positive charge on the $MoO(CH_2)$ fragment of **1d** is clearly higher than the corresponding values for the other systems, indicating a relatively more electron-withdrawing ability of the support in the case of **1d**, compared to **1a**–**1c**. It is explained by the fact that in **1d** the $MoO(CH_2)$ fragment with the formal charge of 2+ substituted two protons from bridge hydroxyl groups, whereas the formation of the **1a**–**1c** models can be regarded as a replacement of one proton from a bridge hydroxyl group and one proton from a less acidic terminal silanol group [58] by the $MoO(CH_2)$ centre (Fig. 1). As the bridge oxygen is less basic than the terminal one, the calculated positive charge on the $MoO(CH_2)$ fragment in **1d** is higher than in **1a**–**1c**.

It was previously shown that, among other factors, higher positive charge on the $MoO(CH_2)$ moiety favours the reactivity of the Mo site toward alkene [25,26]. Actually, for all models considered in this work, the charges on the $MoO(CH_2)$ fragments are relatively high—comparable or higher than the corresponding charges calculated for the most active Mo methylidene species on alumina [25,26] and silica [28].

As the above results indicate that the properties of the Mo methylidene centres **1a**–**1c** are more or less similar, the models **1a** and **1d** have been chosen for further studies of the metathesis activity of the Mo sites in HZSM-5.

Table 3
Selected atomic distances for the minima (**2a**, **4a**, **6a**) and the transition states (**3a**, **5a**) involved in the pathway of ethene metathesis on the Mo methylidene centre **1a**.

	2a	3a	4a	5a	6a
Mo–C1	1.920	1.947	2.024	2.078	2.192
Mo–C3	2.407	2.238	2.083	2.175	2.205
Mo–O1	1.708	1.709	1.715	1.709	1.700
Mo–O2	1.996	2.007	2.006	2.058	2.114
Mo–O3	2.111	2.098	2.082	2.003	2.035
Mo–O4	3.736	3.726	3.776	3.281	2.360
C1–C2	2.650	2.171	1.653	1.590	1.533
C2–C3	1.392	1.441	1.588	1.542	1.530

3.2. Metathesis activity of the Mo centres

All intermediates and transition states involved in ethene metathesis proceeding on the Mo site **1a** are shown in Fig. 2. At the initial stage of the nucleophilic ethene attack, an ethene–molybdenamethylidene complex **2a** is formed. A significant reconstruction of the Mo centre is observed at this step. The Mo–O4 bond, being the weakest among the single Mo–O bonds in the system **1a** (Table 1), is now broken (Table 3), enabling an excellent exposition of the carbene bond toward approaching ethene. The calculated Mo–C3 distance (2.407 Å) for the ethene complex

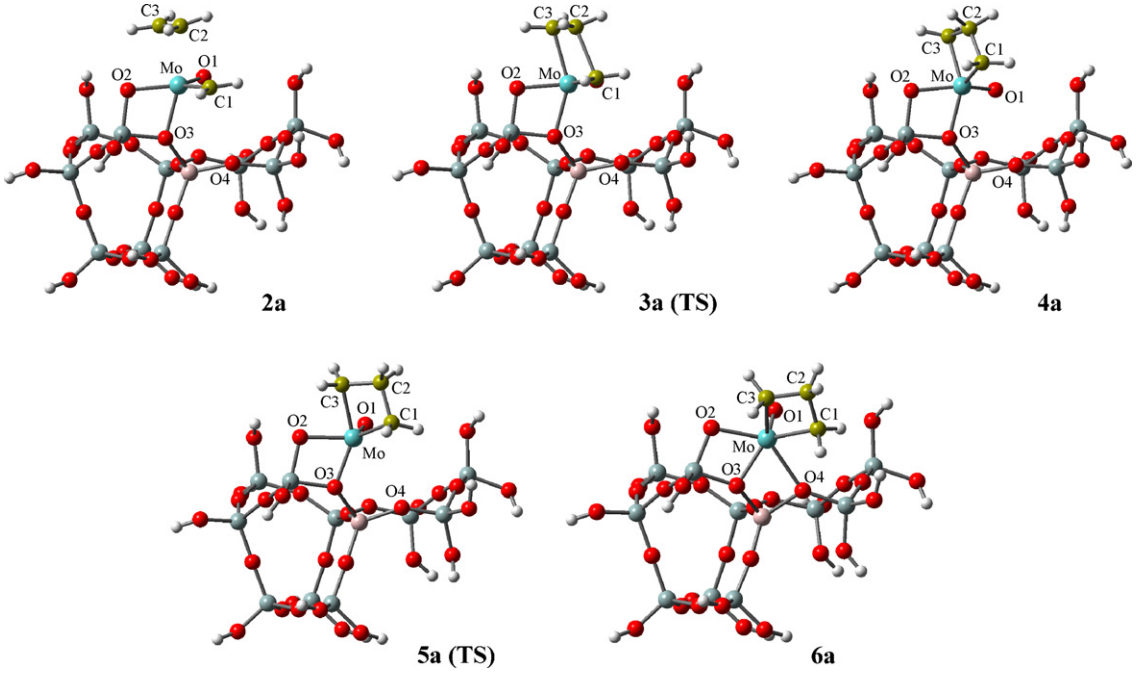

Fig. 2. The minima (**2a**, **4a**, **6a**) and the transition states (**3a**, **5a**) involved in the pathway of ethene metathesis on the Mo methylidene centre **1a**.

is shorter than the corresponding values theoretically obtained for analogous Mo complexes on alumina [25,26] and silica [29]. This indicates a relatively strong interaction between the molybdenum and the ethene molecule, which is additionally confirmed by the elongation of the Mo–C1 bond, compared to **1a** (Tables 1 and 3), and the increase of the C2–C3 distance (1.392 Å), in comparison with a free ethene molecule (1.348 Å).

The ethene complex **2a** can rearrange to the molybdacyclobutane complex **4a** via the transition state **3a** (Fig. 2). Similarly to analogous transition structures investigated previously for the molybdena–alumina and molybdena–silica systems [25–29], the formation of the Mo–C3 bond in **3a** is more advanced than the formation of the C1–C2 bond (Table 3). The molybdacyclobutane intermediate **4a** has a slightly unsymmetrical and puckered ring (Mo–C3–C1–C2 dihedral angle = 172°).

The further step in the metathesis mechanism—cycloreversion—is approximately the reverse reaction for the cycloaddition discussed above. Instead, the molybdacyclobutane **4a** can rearrange to the conformation **6a**, through the transition state **5a** (Fig. 2). This conversion can be considered as a side step of the catalytic cycle of ethene metathesis, because **6a** splits to the Mo methylidene centre and an ethene molecule in two steps, via the intermediate **4a**. The structure **6a** can be described as a molybdacyclobutane complex with a puckered ring (Mo–C3–C1–C2 dihedral angle = 155°) and distorted pentagonal pyramidal geometry. The weak Mo–O4 bond is again recovered in **6a** (Table 3). The ring is almost symmetrical with the Mo–C and C–C distances close to the corresponding bond lengths for theoretically investigated square pyramidal molybdacyclobutanes [17,18,25–29] that are also the secondarily formed molybdacyclobutane complexes.

The energy diagram of ethene metathesis on the Mo site **1a** is presented in Fig. 3. The formation of the ethene complex **2a** is clearly exothermic. Its further conversion to the molybdacyclobutane **4a**, which is the most stable structure on the reaction pathway, is characterised by a very low activation barrier (5 kJ mol^{-1}). However, splitting of the molybdacyclobutane ring to reproduce the Mo methylidene centre **1a** require an energy cost of 62 kJ mol^{-1}. A comparable energy barrier is therefore involved to obtain a new methylidene centre and a free ethene molecule as the product of the metathesis reaction. The calculated Gibbs free energy of the intermediate **4a**, relative to the reactants (Mo methylidene + ethene), is

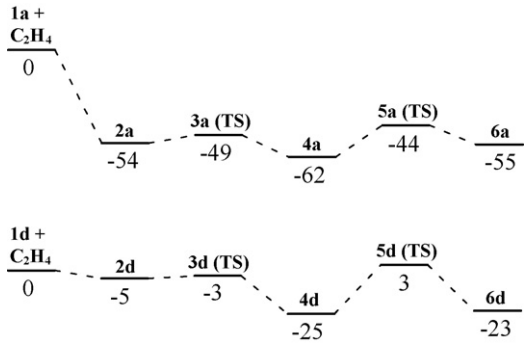

Fig. 3. Energy profiles (kJ mol^{-1}) for ethene metathesis on the Mo methylidene centres **1a** and **1d**.

quite negative (−25 kJ mol^{-1}), indicating a thermodynamically stable structure. Therefore, the Mo methylidene centre **1a** is predicted to be rather moderately active in alkene metathesis.

The transformation of the molybdacyclobutane **4a** to the pentagonal pyramidal structure **6a** is a slightly endothermic step (7 kJ mol^{-1}) with a low activation barrier (18 kJ mol^{-1}). In contrast to alkene metathesis on the molybdena–alumina [25–27] and molybdena–silica systems [28,29], the secondary molybdacyclobutane **6a** does not play an important role in the kinetics of the metathesis reaction, because it is less stable than the primarily formed molybdacyclobutane complex **4a**.

The intermediates and transition states on the pathway of ethene metathesis proceeding on the Mo centre **1d** (Fig. 4) are analogous to those concerning the site **1a**. In the initial ethene complex **2d**, the Mo–O7 bond is broken and the position of the carbene bond enables the attack of an ethene molecule. The Mo–C3 and C1–C2 distances calculated for **2d** are shorter than those for **2a** (Tables 3 and 4). The molybdacyclobutane **4d**, having an almost flat ring (Mo–C3–C1–C2 dihedral angle = 176°), is directly formed from **2d** via the transition structure **3d**. Again, further rearrangement of the primary molybdacyclobutane **4d** to the secondary one **6d** is possible and involves the transition state **5d**. Similarly to **6a**, the six-coordinate molybdacyclobutane complex **6d** has a puckered ring (dihedral Mo–C3–C1–C2 angle = 149°). The molybdenum atom in **5d** and **6d** is again threefold bonded to the surface, like in the start-

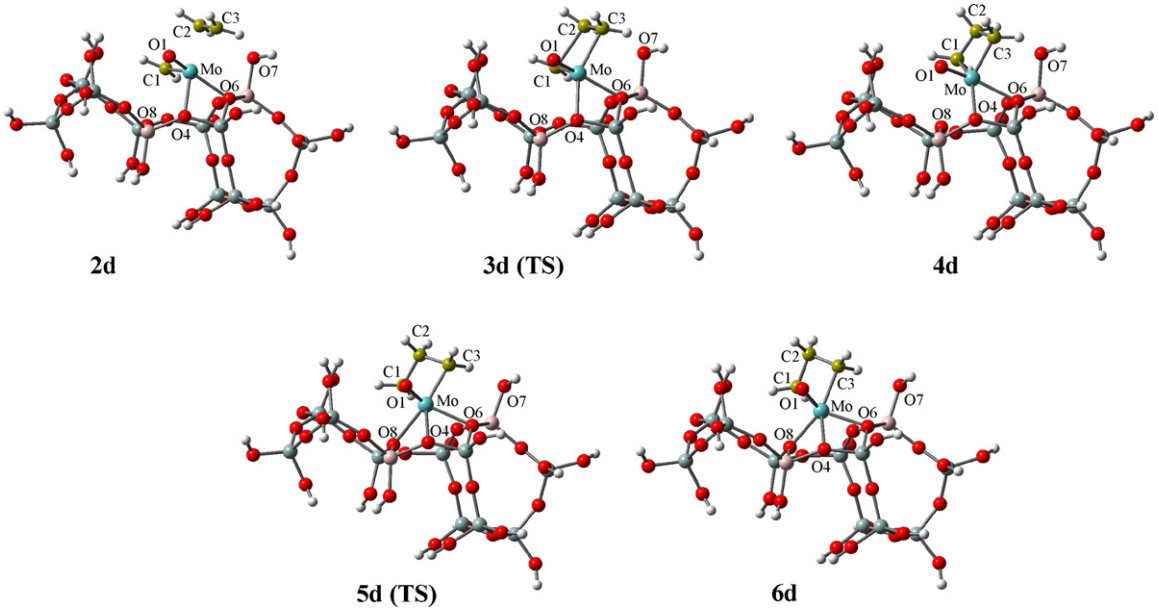

Fig. 4. The minima (**2d**, **4d**, **6d**) and the transition states (**3d**, **5d**) involved in the pathway of ethene metathesis on the Mo methylidene centre **1d**.

Table 4
Selected atomic distances for the minima (**2d**, **4d**, **6d**) and the transition states (**3d**, **5d**) involved in the pathway of ethene metathesis on the Mo methylidene centre **1d**.

	2d	3d	4d	5d	6d
Mo–C1	1.915	1.925	2.060	2.130	2.240
Mo–C3	2.321	2.227	2.036	2.114	2.244
Mo–O1	1.699	1.700	1.703	1.710	1.699
Mo–O4	2.153	2.129	2.142	2.142	2.294
Mo–O6	2.173	2.193	2.211	2.254	2.168
Mo–O7	3.605	3.646	3.616	3.962	3.914
Mo–O8	3.488	3.459	2.633	2.335	2.135
C1–C2	2.507	2.204	1.584	1.553	1.528
C2–C3	1.406	1.439	1.658	1.574	1.526

ing structure **1d**, but here the third bond formed is Mo–O8, instead of the Mo–O7 bond in the Mo methylidene centre **1d** (Figs. 1 and 4).

In contrast to the metathesis pathway on the Mo centre **1a**, the formation of the ethene complex **2d** is hardly exothermic (Fig. 3). The further step leading to the molybdacyclobutane complex **4d** is almost barrierless and involves an energy gain of 20 kJ mol^{-1}. The energy barrier of the cycloreversion step is quite low (25 kJ mol^{-1}), suggesting a high metathesis activity of the Mo site **1d**. Moreover, the intermediate **4d** is unstable relative to the reactants (**1d** + ethene) in terms of the Gibbs free energy, by 14 kJ mol^{-1}. The puckered molybdacyclobutane **6d** is slightly less stable than **4d**, by 2 kJ mol^{-1}, and is formed with the activation barrier of 28 kJ mol^{-1}. Thus, the metathesis step (cycloreversion) is kinetically favoured over the rearrangement of the intermediate **4d** into its isomer **6d**, although the calculated difference in the barriers heights is not very significant.

Therefore, the Mo structure **1d** is a very good candidate for a metathesis-active site. The calculated activation energy of the cycloaddition step is close to zero, whereas the molybdacyclobutane intermediate easily splits to the alkene molecule and the alkylidene site. Moreover, the secondary metallacycle product is less stable than the primary one and its formation is kinetically unfavoured, compared to the desired cycloreversion step. The structure **1d** is predicted to be rather more active in alkene metathesis than theoretically studied Mo sites in molybdena–alumina [25–27] and molybdena–silica [28,29] systems. The structure **1d** can be also considered as a model of the Mo methylidene centre bonded to any silica–alumina support. Thus, the present results are well consistent with the recent experimental findings [11,12] showing that the molybdena–silica–alumina catalysts with low molybdenum loadings exhibit much higher metathesis activity than the molybdena–alumina and molybdena–silica systems.

4. Conclusions

Four different cluster models of Mo(VI) methylidene centres located in the HZSM-5 framework have been proposed and theoretically investigated with DFT. Whereas their geometries are more or less similar, the positive charge on the MoO(CH_2) fragment is clearly higher for the Mo centre having two Al atoms in the vicinity, compared to the models with only one T site occupied by Al atom. This confirms a relatively more electron-withdrawing ability of the support in the former case.

The activity of two selected Mo methylidene centres has been examined by the calculation of the pathway of ethene metathesis. In both cases the cycloaddition step proceeds easily, which can be explained by reduced electron density on the Mo site, as well as by a favourable reconstruction of the methylidene centre at the initial stage of the reaction. On the other hand, the cycloreverse step resulting in ethene release involves a relatively high energy barrier for the Mo centre with one Al site in the neighbourhood, whereas the barrier is quite low for the model with two T sites occupied by Al atoms. Moreover, the key molybdacyclobutane intermediate is a thermodynamically stable species in the first case, but it is unstable in the second case. A secondary molybdacyclobutane structure can be formed as well; however, in both cases it is less stable than the primary metallacycle. Hence, on the basis of these results, a high metathesis activity is predicted if two Brønsted acid sites are replaced by the Mo centre.

The present work confirms the previous findings, both experimental [11,12] and theoretical [25–29], indicating a strong influence of the local properties of the support on the metathesis activity of the Mo sites.

Acknowledgments

This work was partially supported by Polish Ministry of Science and Higher Education (project 4 T09A 056 23). Computing resources from Academic Computer Centre CYFRONET AGH (grants MNiSW/SGI4700/PK/044/2007 and MEiN/SGI3700/PK/021/2006) are gratefully acknowledged.

References

[1] J.C. Mol, J. Mol. Catal. A 213 (2004) 39.
[2] J.L.G. Fierro, J.C. Mol, in: J.L.G. Fierro (Ed.), Metal Oxides: Chemistry and Applications, Taylor & Francis, Boca Raton, 2006, p. 517.
[3] Xu Xiaoding, J.C. Mol, C. Boelhouwer, J. Chem. Soc., Faraday Trans. 1 82 (1986) 2707.
[4] M. Sibeijn, J.A.R. van Veen, A. Bliek, J.A. Moulijn, J. Catal. 145 (1994) 416.
[5] Y. Iwasawa, H. Kubo, H. Hamamura, J. Mol. Catal. 28 (1985) 191.
[6] B.N. Shelimov, I.V. Elev, V.B. Kazansky, J. Mol. Catal. 46 (1988) 187.
[7] A.N. Startsev, O.V. Klimov, E.A. Khomyakova, J. Catal. 139 (1993) 134.
[8] W. Grünert, A.Yu. Stakheev, R. Feldhaus, K. Anders, E.S. Shpiro, Kh.M. Minachev, J. Catal. 135 (1992) 287.
[9] W. Yi, M. Schwidder, W. Grünert, Catal. Lett. 86 (2003) 113.
[10] H. Aritani, O. Fukuda, T. Yamamoto, T. Tanaka, S. Imamura, Chem. Lett. (2000) 66.
[11] J. Handzlik, J. Ogonowski, J. Stoch, M. Mikołajczyk, Catal. Lett. 101 (2005) 65.
[12] J. Handzlik, J. Ogonowski, J. Stoch, M. Mikołajczyk, P. Michorczyk, Appl. Catal. A 312 (2006) 213.
[13] X. Li, W. Zhang, S. Liu, X. Han, L. Xu, X. Bao, J. Mol. Catal. A 250 (2006) 94.
[14] J. Handzlik, P. Michorczyk, J. Ogonowski, unpublished results.
[15] J.-L. Hérisson, Y. Chauvin, Makromol. Chem. 141 (1971) 161.
[16] T.J. Katz, R. Rothchild, J. Am. Chem. Soc. 98 (1976) 2519.
[17] E. Folga, T. Ziegler, Organometallics 12 (1993) 325.
[18] Y.-D. Wu, Z.-H. Peng, J. Am. Chem. Soc. 119 (1997) 8043.
[19] C. Adlhart, P. Chen, J. Am. Chem. Soc. 126 (2004) 3496.
[20] C. Costabile, L. Cavallo, J. Am. Chem. Soc. 126 (2004) 9592.
[21] T.P.M. Goumans, A.W. Ehlers, K. Lammertsma, Organometallics 24 (2005) 3200.
[22] X. Solans-Monfort, E. Clot, C. Copéret, O. Eisenstein, J. Am. Chem. Soc. 127 (2005) 14015.
[23] S. Fomine, M.A. Tlenkopatchev, J. Organomet. Chem. 691 (2006) 5189.
[24] X. Solans-Monfort, J.-S. Filhol, C. Copéret, O. Eisenstein, New J. Chem. 30 (2006) 842.
[25] J. Handzlik, J. Ogonowski, R. Tokarz-Sobieraj, Catal. Today 101 (2005) 163.
[26] J. Handzlik, Surf. Sci. 601 (2007) 2054.
[27] J. Handzlik, P. Sautet, J. Catal. 256 (2008) 1.
[28] J. Handzlik, J. Phys. Chem. B 109 (2005) 20794.
[29] J. Handzlik, J. Phys. Chem. C 111 (2007) 9337.
[30] H. van Koningsveld, H. van Bekkum, J.C. Jansen, Acta Cryst. B 43 (1987) 127.
[31] Y.V. Joshi, K.T. Thomson, Catal. Today 105 (2005) 106.
[32] E. Brocławik, P. Rejmak, P. Kozyra, J. Datka, Catal. Today 114 (2006) 162.
[33] E. Ivanova, M. Mihaylov, H.A. Aleksandrov, M. Daturi, F. Thibault-Starzyk, G.N. Vayssilov, N. Rösch, K.I. Hadjiivanov, J. Phys. Chem. C 111 (2007) 10412.
[34] X. Zheng, Y. Zhang, A.T. Bell, J. Phys. Chem. C 111 (2007) 13442.
[35] A. Chatterjee, D. Bhattacharya, M. Chatterjee, T. Iwasaki, Micropor. Mesopor. Mater. 32 (1999) 189.
[36] K. Teraishi, M. Ishida, J. Irisawa, M. Kume, Y. Takahashi, T. Nakano, H. Nakamura, A. Miyamoto, J. Phys. Chem. B 101 (1997) 8079.
[37] Y. Yokomori, S. Idaka, Micropor. Mesopor. Mater. 28 (1999) 405.
[38] F. Jianfen, B. van de Graaf, H.M. Xiao, S.L. Njo, J. Mol. Struct.: Theochem. 492 (1999) 133.
[39] R. Grau-Crespo, A.G. Peralta, A. Rabdel Ruiz-Salvador, A. Gómez, R. López-Cordero, Phys. Chem. Chem. Phys. 2 (2000) 5716.
[40] K. Sillar, P. Burk, J. Mol. Struct.: Theochem. 589–590 (2002) 281.
[41] S. Sklenak, J. Dědeček, Ch. Li, B. Wichterlová, V. Gábová, M. Sierka, J. Sauer, Angew. Chem. Int. Ed. 46 (2007) 7286.
[42] A.D. Becke, J. Chem. Phys. 98 (1993) 5648.

[43] P.J. Stephens, F.J. Devlin, C.F. Chabalowski, M.J. Frisch, J. Phys. Chem. 98 (1994) 11623.
[44] P.J. Hay, W.R. Wadt, J. Chem. Phys. 82 (1985) 299.
[45] T.H. Dunning Jr., P.J. Hay, in: H.F. Schaefer III (Ed.), Modern Theoretical Chemistry, vol. 3, Plenum, New York, 1976, p. 1.
[46] C. Peng, P.Y. Ayala, H.B. Schlegel, M.J. Frisch, J. Comp. Chem. 17 (1996) 49.
[47] R.S. Mulliken, J. Chem. Phys. 23 (1955), pp. 1833, 1841, 2338, 2343.
[48] A.E. Reed, L.A. Curtiss, F. Weinhold, Chem. Rev. 88 (1988) 899.
[49] E.D. Glendening, A.E. Reed, J.E. Carpenter, F. Weinhold, NBO Version 3.1.
[50] I. Mayer, Chem. Phys. Lett. 97 (1983) 270.
[51] M.J. Frisch, G.W. Trucks, H.B. Schlegel, G.E. Scuseria, M.A. Robb, J.R. Cheeseman, J.A. Montgomery Jr., T. Vreven, K.N. Kudin, J.C. Burant, J.M. Millam, S.S. Iyengar, J. Tomasi, V. Barone, B. Mennucci, M. Cossi, G. Scalmani, N. Rega, G.A. Petersson, H. Nakatsuji, M. Hada, M. Ehara, K. Toyota, R. Fukuda, J. Hasegawa, M. Ishida, T. Nakajima, Y. Honda, O. Kitao, H. Nakai, M. Klene, X. Li, J.E. Knox, H.P. Hratchian, J.B. Cross, V. Bakken, C. Adamo, J. Jaramillo, R. Gomperts, R.E. Stratmann, O. Yazyev, A.J. Austin, R. Cammi, C. Pomelli, J.W. Ochterski, P.Y. Ayala, K. Morokuma, G.A. Voth, P. Salvador, J.J. Dannenberg, V.G. Zakrzewski, S. Dapprich, A.D. Daniels, M.C. Strain, O. Farkas, D.K. Malick, A.D. Rabuck, K. Raghavachari, J.B. Foresman, J.V. Ortiz, Q. Cui, A.G. Baboul, S. Clifford, J. Cioslowski, B.B. Stefanov, G. Liu, A. Liashenko, P. Piskorz, I. Komaromi, R.L. Martin, D.J. Fox, T. Keith, M.A. Al-Laham, C.Y. Peng, A. Nanayakkara, M. Challacombe, P.M.W. Gill, B. Johnson, W. Chen, M.W. Wong, C. Gonzalez, J.A. Pople, Gaussian 03, Revision C.02, Gaussian, Inc., Wallingford, CT, 2004.
[52] R. Dennington II, T. Keith, J. Millam, GaussView, Version 4.1, Semichem, Inc., Shawnee Mission, KS, 2007.
[53] M.J. Rice, A.K. Chakraborty, A.T. Bell, J. Catal. 186 (1999) 222.
[54] J. Dědeček, D. Kaucký, B. Wichterlová, O. Gonsiorová, Phys. Chem. Chem. Phys. 4 (2002) 5406.
[55] J. Dědeček, S. Sklenak, Ch. Li, B. Wichterlová, V. Gábová, J. Brus, M. Sierka, J. Sauer, J. Phys. Chem. C 113 (2009) 1447.
[56] J. Guan, G. Yang, D. Zhou, W. Zhang, X. Liu, X. Han, X. Bao, Catal. Commun. 9 (2008) 2213.
[57] J. Guan, G. Yang, D. Zhou, W. Zhang, X. Liu, X. Han, X. Bao, J. Mol. Catal. A 300 (2009) 41.
[58] P. Hoffmann, J.A. Lobo, Micropor. Mesopor. Mater. 106 (2007) 122.